Hindawi
Journal of Nanomaterials
Volume 2022, Article ID 6889293, 19 pages
https://doi.org/10.1155/2022/6889293

Research Article

Formulation and Development of Adapalene Topical Nanohydrogel Using Different Surfactants and Cosurfactants for Antiacne Activity: *In Vitro* and *Ex Vivo* Evaluation

Vijay Kumar Panthi,[1,2,3] **Saurav Kumar Jha**,[4] **Rudra Pangeni**,[5] **and Keshav Raj Paudel**[5]

[1]*Department of Pharmacy, Tribhuvan University, Sunsari Technical College, Dharan, Sunsari, Nepal*
[2]*Research & Development Department, Asian Pharmaceuticals, Rupandehi, Nepal*
[3]*Research & Development Department, Corel Pharmaceuticals, Rupandehi, Nepal*
[4]*Himalayan Parenteral and Formulations, Janakpur, Nepal*
[5]*Department of Pharmaceutical Sciences, School of Health and Allied Sciences, Pokhara University, Pokhara, Nepal*

Correspondence should be addressed to Vijay Kumar Panthi; nepalivijay7@gmail.com

Received 9 June 2022; Revised 16 August 2022; Accepted 30 August 2022; Published 22 September 2022

Academic Editor: Ruibing Wang

A formulation of an adapalene nanohydrogel (ADP-NH) using different surfactants and cosurfactants for topical application was developed and characterized. The best formulation was obtained with nanohydrogel (NH) containing Tween-80- (NH-Tween-80-) incorporated carbopol-940 and ethanol, 0.67% and 3.00% *w*/*w*, respectively. The optimized formulations of NH-Tween-80, nanohydrogel containing sodium lauryl sulphate (NH-SLS), and nanohydrogel containing glycerol (NH-glycerol) were separately evaluated to examine their *in vitro* and ex vivo permeability characteristics and compared with 0.3% dimethyl sulfoxide (control) solution. The polydispersity index of NH-Tween-80, NH-SLS, and NH-glycerol were found to be 0.264 ± 0.312, 0.382 ± 0.0045, and 0.310 ± 0.412, respectively. All NH formulations showed pH within human skin pH ranges throughout the stability period. The NH-Tween-80 revealed 191.22 μg/mL of ADP permeation through Strat-M® membrane which was statistically significant ($p < 0.05$) compared to NH-SLS, NH-glycerol, and control solution. At 24 h, NH-Tween-80 demonstrated 305.11 μg/mL of ADP permeation in Wistar rat abdominal skin which was 1.99-, 1.56-, and 4.89-fold higher in comparison with NH-SLS, NH-glycerol, and control solution, respectively. Moreover, the ex vivo permeability of NH-Tween-80 was also compared with conventional gel (market sample) which was 3.38-fold greater at 24 h. During the 6th month of accelerated stability analysis, the NH-Tween-80, NH-SLS, and NH-glycerol demonstrated $99.25\% \pm 0.15$, $91.23\% \pm 0.41$, and $96.08\% \pm 0.20$ drug content, respectively. There were no noticeable physical changes observed up to 6 months for NH-Tween-80, while color change was observed in the 1st month and 3rd month of accelerated stability samples of NH-SLS and NH-glycerol, respectively. In this study, only NH-Tween-80 was considered both physically and chemically stable formulation. Therefore, it was concluded that the topical application of ADP-NH containing Tween-80 could be a very promising alternative for the treatment of acne vulgaris.

1. Introduction

Acne vulgaris is an inflammatory ailment associated with the pilosebaceous unit and represents severe scarring of both physical and mental conditions that impact the quality of life [1]. The seriousness of this condition could be assumed from the statistical data, which revealed approximately 70–80% of teenagers/adolescents suffered this disorder. Nevertheless, the therapy for acne is challenging mainly because of uncertainty about the effective outcomes and the requirement of longer treatment durations. Medications via topical administration are commonly favored before curing normal to

moderate acne. Among various derivatives of vitamin A, retinoids are generally recommended for treating comedonal acne [2]. Adapalene (ADP) belongs to the third-generation class of retinoids, which reveals various therapeutic effects, including anti-inflammatory, antiseborrheic, and keratolytic. ADP has been found beneficial for treating acne by balancing the differentiation of skin and oil synthesis and is found to be efficacious in several skin disorders such as keratosis pilaris. Chemically, ADP is 6-[3-(1-adamantyl)-4-methoxyphenyl] naphthalene-2-carboxylic acid and the molecular formula C28H28O3 g/mol. Physically, the color of ADP varies from white to off-white, mainly in crystalline form, and has no practical solubility in aqueous solvents [3]. Therefore, current ADP conventional topical therapy for acne is criticized due to unsatisfactory patient compliance, uncertain pharmacokinetics of skin, and serious adverse effects. Furthermore, commercially available ADP preparations such as Differin and Adiff gel are reported to reveal critical side effects including erythema, burning, dryness, skin peeling, and itching, which may minimize the utilization of ADP [4–6]. To decrease the aforementioned adverse reactions, users need to minimize sunlight exposure, resist higher temperatures, and apply moisturizers. Thus, new drug administration approaches should exhibit the ability to counteract these drug-related reactions and enhance patient compliance in addition to effective drug delivery.

The therapeutic benefits of acne could be achieved by developing an ADP formulation having improved physicochemical properties and controlled and targeted drug release at the pilosebaceous unit. Nanoparticles (NPs) are considered the most appropriate choice mainly for targeted topical administration of various drugs, such as ADP for treating acne [7]. Based on particle size, physicochemical characteristics, and surface charge, NPs could penetrate the deeper skin layers. Additionally, it might be declined on the surface of the skin and promotes to emit the active pharmaceutical ingredients (APIs) which have been incorporated. Several *in vitro* and *in vivo* studies have demonstrated that particle sizes smaller than 3 μm are randomly distributed in the stratum corneum (SC) and particle size above 10 μm remains on the outermost part of the skin [8]. Briefly, the desired site to treat acne and the pilosebaceous unit contains the hair shaft, hair follicle, and attached arrector pili muscles in addition to sebaceous glands. The hair follicle is an introversion of the external parts of skin called epidermis associating up to the dermis, providing a greater surface area for absorption of APIs [9]. Furthermore, topically administered nanoparticulate formulation of drugs generally deposits in hair follicles which are removed progressively by following a few intermediate processes, including hair growth and flow of sebum in an outward direction [10].

This research was aimed at formulating an ADP-incorporated topical nanohydrogel (NH) system to enhance skin permeation and target hair follicles for site-specific delivery. Firstly, the ADP was solubilized in ethanol (99.9%). Next, to further increase the solubility-permeability and drug loading capacity of different surfactants/cosurfactants such as Tween-80, polyethylene glycol-(PEG-) 400 polypropylene glycol (PG), sodium lauryl sulphate (SLS), benzylkonium chloride (BC), glycerol, and sodium docusate were used, and then, the solubilized mixture was incorporated into the hydrogel system prepared of pharmaceutically acceptable thickening agent carbopol-940. After that, the *in vitro* permeabilities of ADP nanohydrogel (ADP-NH) across the artificial membrane and the abdominal skin of Wistar rat as an ex vivo model were examined. Moreover, till date, various researches have been published associated with the preparation and uses of hydrogel formulation. A study done by Li et al. has prepared multiresponsive biodegradable cationic nanogels for treatment of tumors. This study has been revealed that the drug-incorporated nanogel formulation completely eliminated advanced tumors and remarkably hinder recurrence [11]. Furthermore, a study carried out by Ding et al. also formulated chitosan nanogels for selective intracellular drug delivery, and their research reported excellent biocompatibility and selective therapeutic efficacy against cancer cells [12]. Additionally, Luo et al. also studied 3D-printing hydrogel scaffolds as a prospective therapy for breast cancer and tissue repair [13]. Furthermore, Ghasemiyeh and Mohammadi-Samani and Sun et al. also prepared curcumin-loaded poly(-lactic-co-glycolic acid) (PLGA) nanoparticles to examine the antipsoriasis activity via enhancement of topical penetration, and in that study, the antipsoriasis activity was significantly ameliorated in mice [14, 15].

2. Materials and Methods

2.1. Materials. All the required materials were obtained from reliable sources; PG, ethanol, dimethyl sulfoxide (DMSO), PEG-400, BC, glycerol, and Tween-80 were procured from Thermo Fisher GmbH, Karlsruhe, Germany. ADP was purchased from BAL Pharma Ltd., and carbopol-940 was obtained from Corel Pharma Chem, Ahmedabad, India. The SLS, methyl paraben sodium (MPS), propyl paraben sodium (PPS), sodium docusate, disodium edetate, and triethanolamine were received as a free sample from the Colorcon Asia Pvt. Ltd, industrial estate, Goa, India.

2.2. Animals. Wistar rats having an approximate weight range from 150 to 200 g were housed in the animal house of Sunsari Technical College, Department of Pharmacy, Sunsari, Nepal, and selected for ex vivo irritation and permeability evaluation. These animals were placed by appropriately maintaining standard conditions of temperature (23 ± 2°C), humidity (50 ± 5) RH, and 12/12 h light and dark cycles. The animals were provided both food and water in very convenient access. The experiments were carried out as per the ethical norms specified by the institutional committee.

2.3. Solubility Study of ADP and Standard Curve Determination. At first, the ADP solubility in several surfactants and cosurfactants was examined by pouring sufficient ADP in microcentrifuge tubes consisting of 4 mL of the preferred excipients like PEG-400, Tween-80, SLS, and glycerol. The vials, after sealing, were vortexed on a nutating mixer for 72 hours at room temperature (25°C). Subsequently,

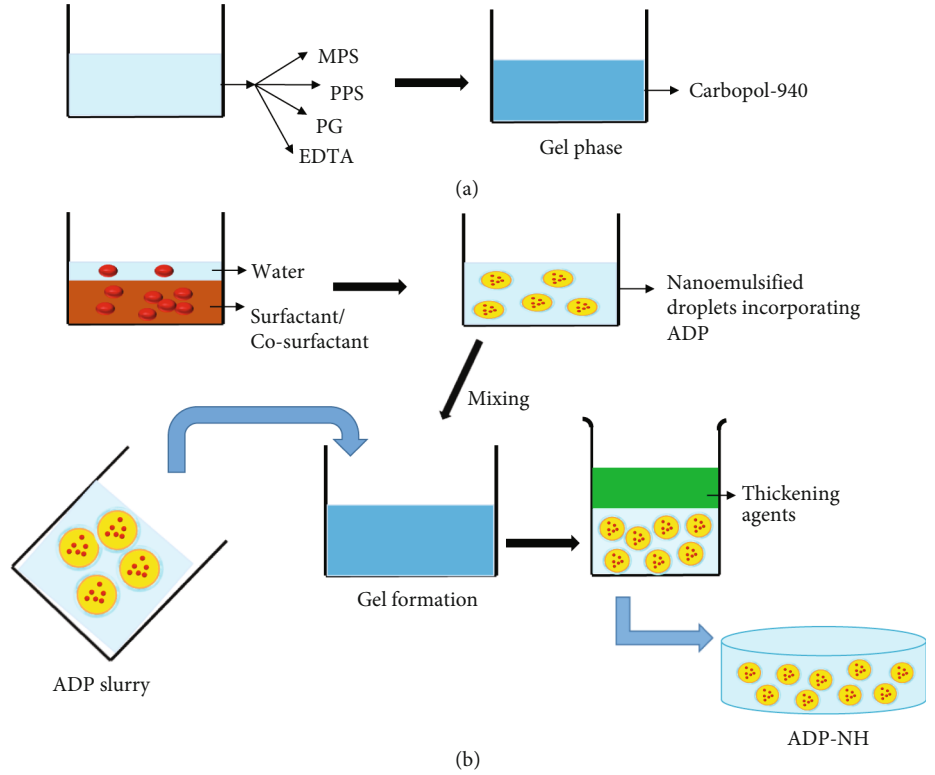

Figure 1: Diagrammatic representation of ADP-NH formulation.

centrifugation was done for 15 minutes at 5000 rpm to eliminate the amount of undissolved drug. At first, supernatants were separated by filtration using a membrane filter having with a pore size of 0.45 μm, and finally, methanol was used to dilute. The proportion of the dissolved drug in each chosen vehicle was determined by HPLC (Agilent 1260) and UV-Vis detector (Agilent Technologies, Santa Clara, USA) at 235 nm, the analytical column has the dimension of 4.6 mm $\times$ 25 cm and 5 μm packing L1. Then, mobile phase is composed of acetonitrile, tetrahydrofuran, trifluoroacetic acid, and water (43 : 36 : 0.02 : 21 v/v) in addition to injection volume and flow that rate were 20 μL and 1 mL/min, respectively [16]. Moreover, in this study, the calibration curve of ADP was prepared by injecting different concentrations of ADP (16, 18, 20, 22, and 24 μg/mL) in HPLC according to the method described above. Finally, the coefficient correlation (R^2), slope, and intercept were calculated.

2.4. Preparation of Topical Nanohydrogel. To develop topical NH, two different phases (gel phase and active phase) were prepared separately. Firstly, purified water (sufficient to soak) was weighed, and disodium EDTA, MPS, PPS, and PG were dissolved with continuous stirring until a clear solution appeared. Then, dispersed carbopol-940 was allowed to soak overnight before obtaining gel-like consistency. Moreover, for preparation of the active phase, the remaining quantity of purified water was heated separately at 90 to 100°C. Sodium docusate, surfactant, and cosurfactant were separately dissolved with continuous stirring and then allowed to cool until the temperature reached 40 to 45°C. Furthermore, ADP was dispersed with regular stirring for about 15 minutes to get a clear ADP solution. In addition, to mix the two phases, ethanol was added dropwise in the gel phase with regular stirring for about 10 minutes, and ADP slurry was transferred into the apparatus containing the gel phase with a continual stirring of about 30 minutes. Then, triethanolamine was added following continuous stirring for 15 minutes. Further homogenization and colliding were done before enhancing the smoothness of gel's smoothness and obtaining a gel in nanoform (Figure 1). The detailed list of excipients and their quantity used was demonstrated in the formulation chart (Table 1). After adding ADP active phase to the gel phase, F1, F2, and F3 were immediately converted into liquid. Therefore, these formulations were not thoroughly studied.

2.5. Characterization of ADP Topical Nanohydrogel

2.5.1. Appearance. The NH formulations were observed visually against the light to evaluate the homogeneity and optical transparency. In addition, monophasic systems were also evaluated to detect any insoluble drug components or solid particulates. Furthermore, the shape and surface morphology of formulations was examined by transmission electron microscopy (TEM). Furthermore, to assess the morphological study, the staining of NH sample was performed using a 2% phosphotungstic acid solution. Then, a drop of the formulation was kept onto a copper grid coated with a carbon film and allowed for drying under infrared radiation before viewing under the microscope. The filter

Table 1: Different ADP-NH formulations.

Ingredients (gm/tube)	F1	F2	F3	F4	F5	F6
Adapalene	0.015	0.015	0.015	0.015	0.015	0.015
Carbopol-940	0.1555	0.1555	0.1555	0.100	0.105	0.113
PG	0.030	—	—	—	—	—
SLS	—	—	—	—	—	0.030
Tween-80	—	—	—	0.030	—	—
Glycerol	—	—	—	—	0.030	—
PEG-400	—	—	0.030	—	—	—
BC	—	0.030	—	—	—	—
Sodium docusate	0.008	0.008	0.008	0.008	0.008	0.008
PG	2.400	2.400	2.400	2.400	2.400	2.400
Disodium Edetate	0.030	0.030	0.030	0.030	0.030	0.030
MPS	0.027	0.027	0.027	0.027	0.027	0.027
PPS	0.003	0.003	0.003	0.003	0.003	0.003
Ethanol (99.9%)	0.200	0.250	0.400	0.450	0.350	0.300
Triethanolamine	0.0275	0.0275	0.0275	0.0275	0.0275	0.0275
Purified water	12.104	12.054	11.904	11.910	12.005	12.047
Total	15.000	15.000	15.000	15.000	15.000	15.000

Table 2: Solubility (mean ± SD) of ADP.

Surfactants	Solubility (mg/mL)	Cosurfactants	Solubility (mg/mL)
Tween-80	32.40 ± 0.45	PEG-400	19.17 ± 0.55
SLS	11.52 ± 0.37	Glycerol	28.77 ± 0.24
BC	0.62 ± 0.31	PG	4.10 ± 1.02

Values are expressed as mean ± SD ($n = 3$).

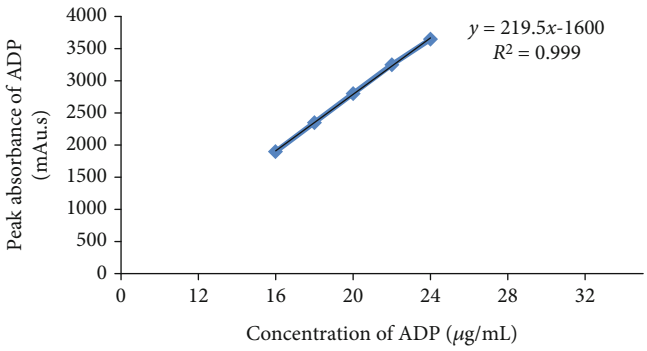

Figure 2: Standard calibration curve of ADP.

paper was used to eliminate the excess matters, and the grid was viewed by TEM (H7600, Hitachi, Tokyo, Japan).

2.5.2. Particle Size, Polydispersity Index (PDI), and Zeta Potential Assessment. The droplet size, particle size distribution, and zeta potential of optimized three formulations were assessed by Zetasizer Nano ZS (Malvern instruments, Malvern, UK). To determine these parameters, NH containing ADP was diluted with deionised water (1 : 50), followed by vortex mixing for 2 min. The effect of light scattering was observed at 25°C with a fixed angle of 90°C, and each sample was measured in triplicate.

2.5.3. Evaluation of pH. In this study, mean pH was measured with a digital pH meter (Ohaus, Model-Starter 3100C), and before carrying out the measurement, standardization was done with pH 4 and 7 buffer. A 5.0 g sample of NH containing ADP was accurately weighed, and the dilution was done with deionised water containing 95 mL. Then, the pH of the active phase and NH containing ADP were determined. Each sample was measured in triplicate.

2.5.4. Conductivity Evaluation. The conductivity of the ADP phase and NH formulations were analyzed with a digital pH meter (Ohaus, Model-Starter 3100C). The glass electrode was calibrated with the solution specified for the apparatus having two different values of pH, such as 4.00 and 7.00. The evaluation of conductivity was performed in microsiemens per centimeter (μS/cm). During measurement, the sample to be assessed was left for approximately 15 minutes to maintain equilibrium. Moreover, conductivity determination of formulation was performed in triplicate, and the mean value of each preparation was calculated.

2.5.5. Viscosity Measurement. A Brookfield Viscometer (Brookfield DV-2+pro) with spindle S64 was used to examine the viscosity of optimized preparations. In this study, the final formulations were poured into the beaker and then allowed to settle down at 25 ± 1°C for 30 minutes before measuring. Subsequently, the spindle was perpendicularly positioned in the centre of NH, then cautiously observed and ensured that the spindle was not touched by the lower part of the jar, and revolved for 10 minutes at a speed of 60 rpm; then, the viscosity value was noted down [17].

Table 3: Particle size, PDI, and zeta potential (mean ± SD) of different formulations.

Formulation	Zeta size (nm)	PDI	Zeta potential (mV)
NH-Tween-80	76.53 ± 0.115	0.264 ± 0.312	−7.63 ± 1.12
NH-SLS	91.27 ± 0.257	0.382 ± 0.0045	−11.45 ± 2.24
NH-glycerol	84.59 ± 1.17	0.310 ± 0.412	−14.21 ± 1.67

Values are expressed as mean ± SD ($n = 3$).

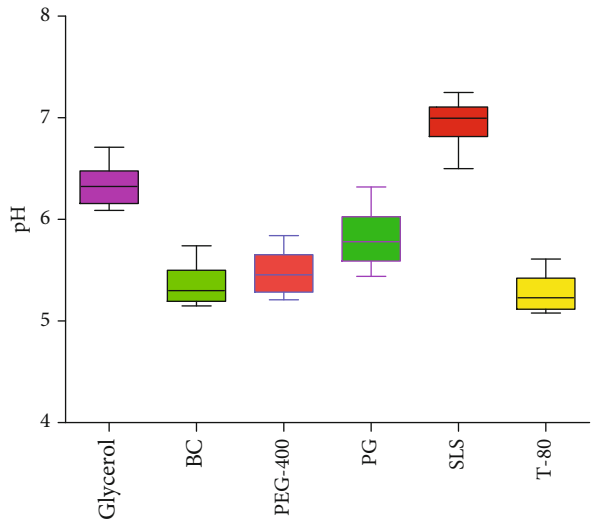

Figure 3: Box plot representation of pH value of Active (ADP) phase in surfactants and cosurfactants.

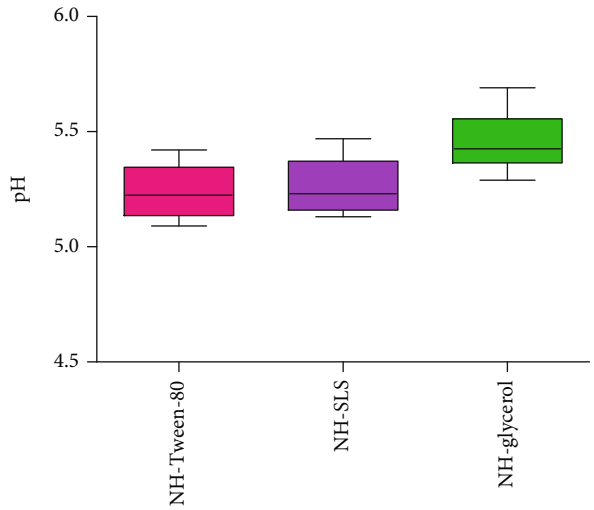

Figure 4: Box plot representation of pH value of NH formulations.

2.5.6. Spreadability. In this study, to determine the formulations spreadability, accurately weighed 1 g of NH sample was placed within 1 cm diameter of a premarked circle on a glass plate, and above this, another glass plate was added. A weight of 20 g was allowed for resting on the upper glass plate for 5 min. The area of diameter increment owing to the spreading of the gels is recorded, and the average diameter was finalized. Finally, spreadability was calculated by applying the below-mentioned formula:

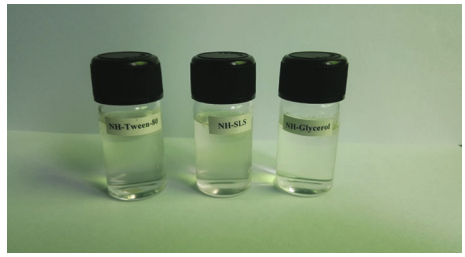

Figure 5: Photographs of ADP-optimized NH formulations on day 1.

$$S = \frac{m \cdot l}{t}, \quad (1)$$

where S stands for spreadability, m denotes weight added on the upper slide, l defines the length of upper the slide, and t denotes the time taken [18].

2.6. Determination of ADP Assay in Optimized NH Formulations. To determine the ADP assay in NH formulations, prepared 0.25 mg/mL of ADP standard stock solution and 20 μg/mL of ADP standard solution were diluted with mobile phase consisting of acetonitrile, tetrahydrofuran, trifluoroacetic acid, and water (43 : 36 : 0.02 : 21 v/v) having injection volume and flow rate were 20 μL and 1 mL/min, respectively. The ADP content in each NH formulation was quantified by applying the HPLC method described in Section 2.2. Each NH formulation placed in both room temperature and accelerated stability chamber was analyzed for up to 6 months. The acceptance criteria for formulated gel was 90.0%-110.0% [19].

2.7. Dermal Irritation Study. The ability and degree of all optimized formulations causing skin irritation were examined on the uninjured skin of Wistar albino rats ($n = 6$). These animals were categorized into four groups, and their skin was attached to the dorsal side of each right and left portion of an individual rat just before one day of the experiment. The left portion of the animal was marked as a negative control, whereas the right side was considered a test to be conducted site. Each optimized NH (NH-Tween-80, NH-SLS, and NH-glycerol) containing a thin layer was topically applied on the test site of individual rat of their representing group. The section to be tested was masked with a gauze patch and plastic sheet. The 0.9% saline solution was applied to control parts and covered the same as previously described and then allowed to expose for 24 h. The next day, the materials used to cover were dispatched cautiously. Additionally, the test section was clean with purified water and allowed for drying. Subsequently, the rats were evaluated to examine the occurrence of any skin reactions such as erythema and edema following the scoring system of Draize dermal irritation. This scoring system is divided into

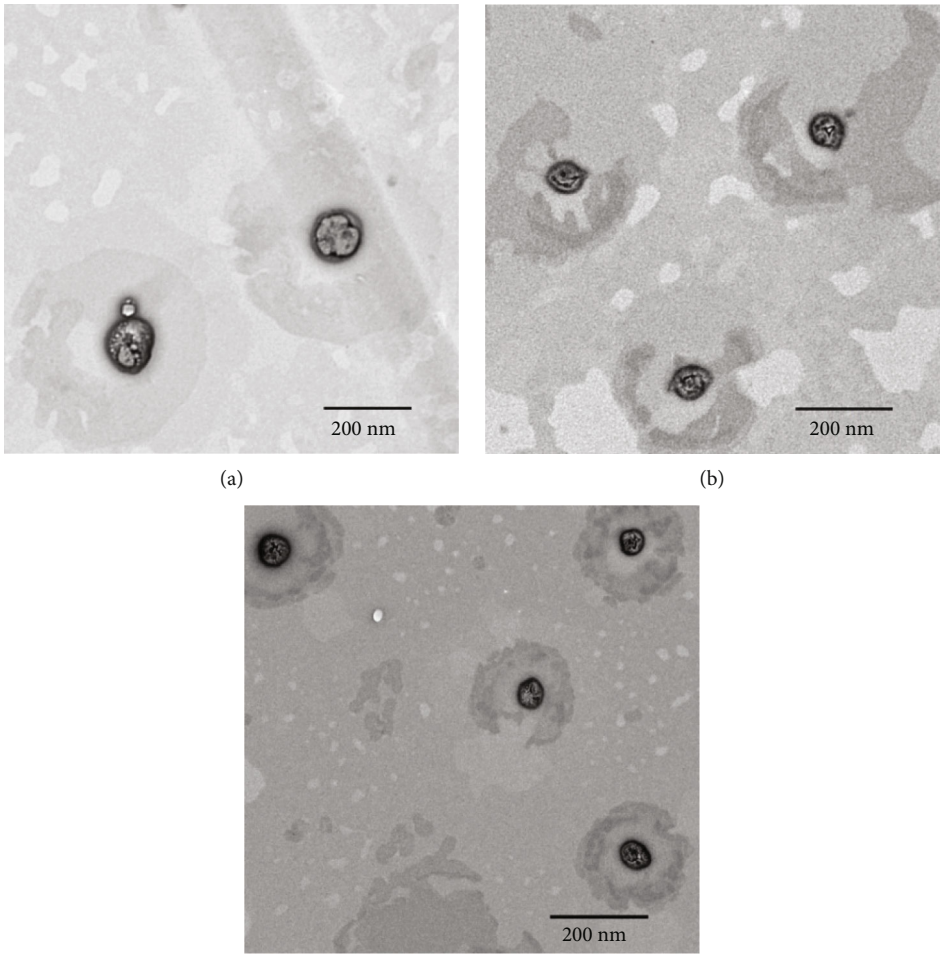

(a) (b) (c)

Figure 6: Transmission electron micrographs of optimized formulations: (a) NH-Tween-80, (b) NH-SLS, and (c) NH-glycerol.

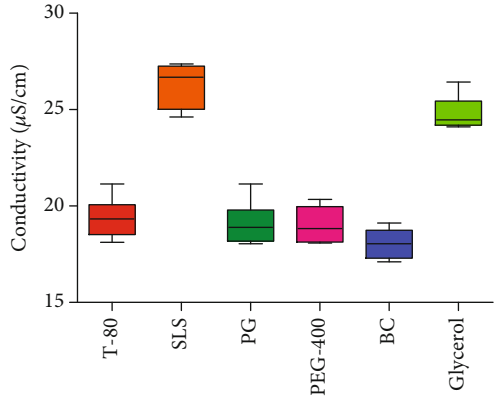

Figure 7: Box plot representation of conductivity value of Active (ADP) phase in surfactants and cosurfactants.

five different categories where 0 stands for the absence of edema or erythema; 1 means hardly appeared edema or erythema; 2 defines clearly identified erythema or normal edema; 3 denotes the range of edema and erythema from moderate to severe; and finally, 4 denotes the very sensitive edema or erythema) at scoring durations of 24, 48, and 72 h after topical delivery to determine the dermal toxicity [20, 21].

2.8. Permeability Study

2.8.1. In Vitro Artificial Transdermal Membrane Permeability. To evaluate the skin permeation of ADP formulations, a synthetic membrane (Strat-MVR; EMD Millipore, Temecula, CA, USA) was used after assembling with Franz diffusion cell system (Labfine, Gyeonggi-do, Republic of Korea) for the estimation of transdermal membrane permeability as an *in vitro* study. Each Strat-MVR disc having a 25 mm diameter was set up on the receiver compartment with a diffusion area of 0.785 cm^2. The NH containing ADP was diluted with deionised water (1 : 50), followed by vortex mixing for 2 min. After completion of donor compartment assembling, 5 mL of phosphate-buffered saline (PBS; pH 7.4) was poured into the receiver compartment, and then, cells were left for the attainment of equilibrium for minimally 60 minutes to ensure the hydration of the membrane. Afterward, 1 mL containing each NH-Tween-80, NH-SLS, and NH-glycerol and ADP in 0.3% DMSO (Control solution) was added to the donor compartment.

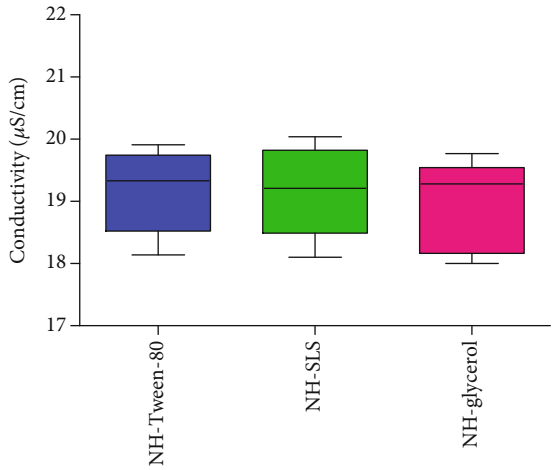

Figure 8: Box plot representation of conductivity value of NH formulations.

Table 4: Spreadability and viscosity of different formulations.

Formulation	Spreadability (mm)	Viscosity (cPs)
NH-Tween-80	7.5 ± 0.37	2257 ± 0.41
NH-SLS	5.69 ± 0.52	2495 ± 0.29
NH-glycerol	6.22 ± 0.44	2372 ± 0.54

Values are expressed as mean ± SD ($n = 3$).

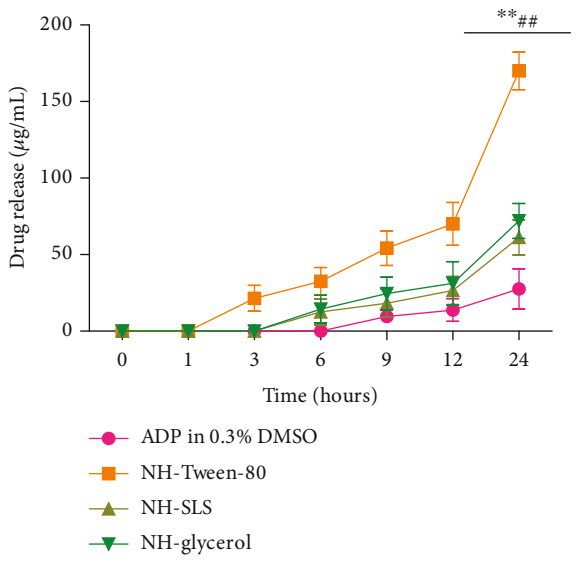

Figure 9: Mean (±SD) amount of ADP permeated across Strat-M® artificial transdermal membrane ($n = 3$) from NH formulations (NH-Tween-80, NH-SLS, and NH-glycerol) and ADP in 0.3% DMSO: $^{**}p < 0.05$ vs. ADP in 0.3% DMSO solution; $^{\#\#}p < 0.001$ vs. NH-SLS.

The stirring was continuously allowed in the receiver part at 600 rpm of the heating system to achieve a surface temperature of the membrane of 32°C until the completion of the test. Then, the receptor phase consisting of 300 μL of volume was taken after completing 12 and 24 hours, and each volume of withdrawn was compensated by adding the same volume of freshly prepared PBS (pH 7.4). Then, filtration of collected samples was performed membrane filter (0.45 mm, polyvinylidene fluoride, PVDF), and then, the amount of ADP permeated via the artificial membrane was quantified with HPLC-facilitated C18 column (4.6 mm × 25 cm and 5 μm packing L1). Finally, the concentration of ADP permeated was measured using an HPLC method mentioned in Section 2.2.

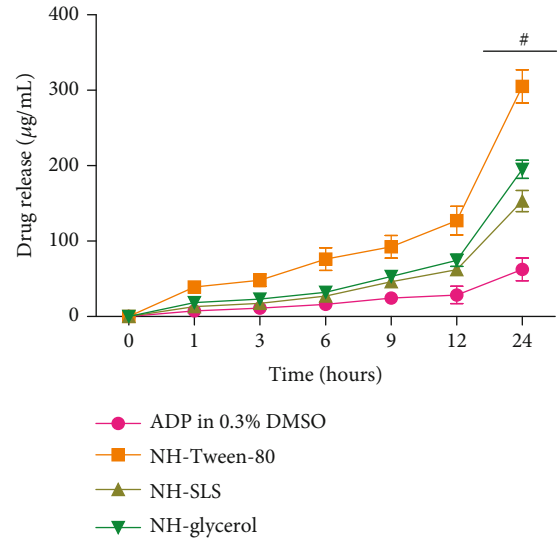

Figure 10: Mean (±SD) amount of ADP permeated across rat abdominal skin ($n = 3$) from NH formulations (NH-Tween-80, NH-SLS, and NH-glycerol) and ADP in 0.3% DMSO: $^{*}p < 0.05$ vs. ADP in 0.3% DMSO solution.

2.8.2. Ex Vivo Drug Permeation. To assess skin permeability of ADP topical NHs, the abdominal hair of Wistar male albino rats was removed using a razor upon sacrificing by spinal dislocation. The skin of the abdomen was removed by surgery, and the remaining fat adhered on the subcutaneous site was thoroughly cleaned. Subsequently, the epidermis part was isolated from the dermis by soaking the full thickness skin in solution containing sodium bromide with a concentration of 2 M about 6-8 h. The portion of the epidermis was adequately cleaned with purified water and allowed to store in the freezer to use further. Furthermore, regarding the ex vivo permeation research, skin hydration was done for one hour before the Franz diffusion cell was adjusted with the SC towards the side of the donor compartment. After assembling the donor compartment, 5 mL of phosphate-buffered saline (PBS; pH 7.4) was poured into the receiver compartment. The NHs containing ADP were diluted with deionised water (1 : 50), and then, the solution was vortexed for approximately 2 min. Then, NH solution containing 1 g was poured on the SC part in the donor section. The stirring was done at 600 rpm in the acceptor region and heated to ensure the maintenance of the surface at 32 ± 0.5°C until the completion of the experiment [22]. Then, 300 μL of sample solution was withdrawn from the diffusion

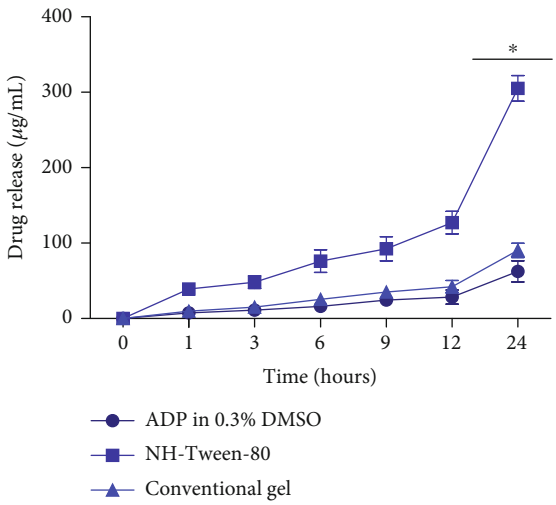

Figure 11: Mean (±SD) amount of ADP permeated across rat abdominal skin ($n = 3$) from NH-Tween-80, conventional gel, and ADP in 0.3% DMSO: $^{*}p < 0.05$ vs. conventional gel and control solution.

cell of the receiver compartment at different durations including 1, 3, 6, 9, 12, and 24 hours, and the volume was adjusted by adding the same volume of freshly prepared PBS (pH 7.4). The filtration of each collected sample was done using membrane filter (0.45 mm, PVDF), and the permeated concentration of ADP through the abdominal skin of Wistar rat was assessed using HPLC at 235 nm by applying isocratic elution method, as described in Section 2.2.

2.9. In Vitro Antibacterial Study

2.9.1. Minimum Inhibitory Concentrations (MIC). The potentiality of different optimized ADP-NH formulations to exhibit bacterial growth inhibition at lower concentrations was assessed using an agar dilution assay. The serial dilutions of NH-Tween-80 in Mueller-Hinton (MH) agar have a final ADP concentration between 0.5 and 4.0 μg/mL. Moreover, to further assess the dose-dependent antibacterial effect of the formulation, ADP concentrations including 0.15, 0.25, 1.0, and 1.25 μg/mL and control group (NH without adding Tween-80) were also used. The MH agar medium was prepared as per instructions provided by the manufacturer, and the autoclaving was performed at 20 psi for 20 minutes. After autoclaving, the agar medium was allowed to cool in a water bath approximately at 40-45°C. Moreover, 60 mL of the cooled agar medium was carefully added to the prepared Petri dish having a diameter of 150 × 15 mm. The agar was cooled at room temperature and placed in a refrigerator (2-8°C) until used. The surface of the agar plates consisting different concentrations of NH-Tween-80 was inoculated with standard inoculums (optical density 0.08-01 at 625 nm wavelength) of Staphylococcus epidermidis overnight. The cultured plates were allowed to incubate for 24 h at 37°C. Afterwards, end points for ADP were evaluated by placing plates on a dark background, and noticing the lowest concentration inhibiting visible growth is considered in the MIC [23].

3. Accelerated Stability Studies

In this research, the stability study of optimized formulations was performed as per the International Conference on Harmonization (ICH). In general, the guidelines recommended by ICH for long-term and accelerated storage conditions are 25°C ± 2°C/60%relative humidity (RH) ± 5% RH and 40°C ± 2°C/75%RH ± 5% RH, respectively. If appropriate, an intermediate storage condition (30°C ± 2°C/65%RH ± 5%RH) is specified according to ICH guidelines [24]. In this study, the formulation filled in polylaminated tube was exposed to accelerated stability testing for six months following ICH norms at a temperature (40 ± 2°C) and relative humidity of 75 ± 5%. The samples were analyzed at different durations such as 1st month, 3rd month, and 6th month for the change in pH, color, phase separation, and drug content by procedure stated earlier. Any noticeable changes observed in these parameters were recorded. Each test was performed in triplicate, and both average values and standard deviation were calculated.

4. Statistical Analyses

In this study, statistical analyses were carried out using GraphPad Prism 5.0 (GraphPad Software, Inc., San Diego, CA). The one-way analysis of variance (ANOVA) followed by Tukey's multiple comparison test was used to evaluate the data. A $p < 0.05$ was applied to show statistical significance. All findings are calculated as a mean ± standard deviation.

5. Results and Discussion

5.1. Solubility of ADP and Preparation of Standard Curve. To formulate a NH system incorporating ADP for topical route, it is required to possess a good solubility as merely solubilized drugs can permeate via the skin. Solubility study of ADP in several surfactants and cosurfactants was performed, and the values are shown in Table 2. In this study, ADP showed the highest solubility in Tween-80 (32.40 ± 0.45 mg/mL) followed by glycerol and PEG-400. The SLS and BC revealed 11.52 ± 0.37 mg/mL and 0.62 ± 0.31 mg/mL of solubility, respectively. Additionally, to prepare a standard curve, the average area received from HPLC analysis was organized in accordance with different concentrations of ADP. This parameter revealed a concentration-dependent interrelationship between 16 and 24 μg/mL (Figure 2). Moreover, in this concentration range, the R^2 and regression equation of ADP were 0.999 and $y = 219.5x - 1600$, respectively, revealing a linear interconnection between the concentration of analytes and peak area.

5.2. Optimization of Nanohydrogel Formulations. As suggested in the literature, the excipients were selected based on safety, solubility, and miscibility with ADP. After the finalization of six solvents, the solubility of ADP was carried out with the selected surfactants. Furthermore, as the solubility data shown in Section 5.1, the ADP exhibited higher solubility in Tween-80, followed by glycerol and SLS. In

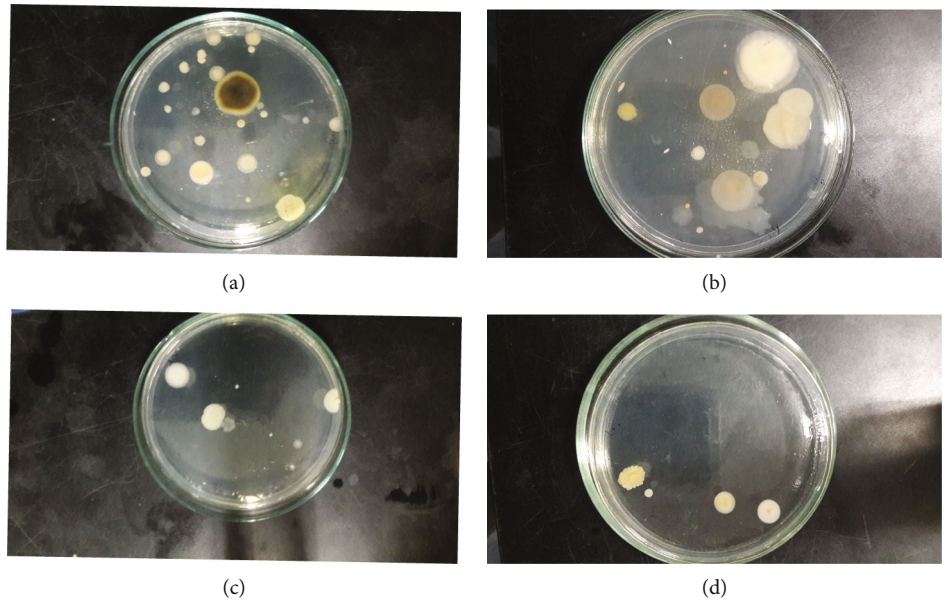

Figure 12: Dose-dependent effect of NH-Tween-80 against S. epidermidis: (a) 0.5 μg/mL, (b) 1.5 μg/mL, (c) 3.0 μg/mL, and (d) 4.0 μg/mL.

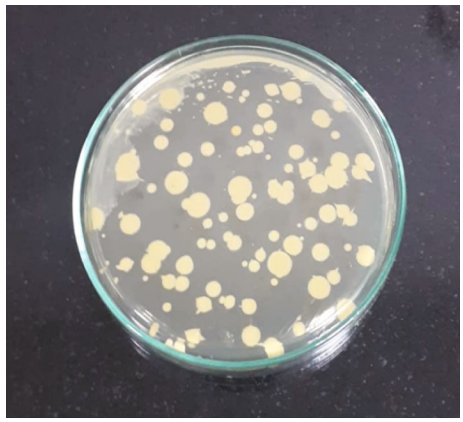

Figure 13: Antibacterial effect of control group.

addition, to examine the possibilities of NH formulation, initially, ADP was tried with all surfactants. However, after adding ADP active phase to the gel phase, the gel consistency of F1 (containing PG), F2 (containing BC), and F3 (containing PEG-400) was immediately converted into a liquid state; thereby, these formulations were stopped for further processing and detailed evaluation. On the contrary, this type of problem did not appeared with formulations containing surfactants such as Tween-80, SLS, and glycerol, which means that after the addition of the ADP active phase to the gel phase, the proper gel consistency was observed, and the proportion of ADP solubility in these surfactants was also better. Thus, ADP-NH consisting of Tween-80, SLS, and glycerol was optimized for detailed evaluation. Additionally, the overall technique of NH preparation was described in Section 2.4.

The surfactant can be utilized alone or in combination, but they have better solubilization potentiality. Surfactants are categorized into various classes based on charge and their nature, such as nonionic, zwitterionic, cationic, and anionic surfactants. Moreover, various studies have been reported that the surfactants such as Tween-80, PEG-400, PG, SLS, BC, glycerol, and sodium docusate are widely used in lotions, creams, and gel formulations and labeled as safe FDA for cosmetic use [25]. Nevertheless, excipients like Tween-80, PEG-400, PG, and SLS are widely reported to be used in conventional as well as novel oral formulations generally regarded as safe. Due to the poor solubility of ADP, it was solubilized in ethanol, and further to inhibit the precipitation of ADP from the ethanol, the amphiphilic surfactants/cosurfactants like PEG-400 PG, Tween-80, and glycerol were used. To enhance the solubility-permeability and stability of ADP-loaded nanodroplets in gel, ionic surfactants like SLS, BC, and sodium docusate were also used, and NH-formulation of ADP (F1-F6) was prepared [26]. In addition, all excipients used in this study are nonirritant. In brief, it has been suggested that nonionic surfactants including Tween-80 are widely accepted as a good choice because of their less toxicity and low irritant compared to ionic surfactants [27]. In addition, PEG 400 is an FDA-approved polymer for drug delivery systems because of its safety and tolerance when administered to the body by different routes. To improve the efficacy of topical and transdermal delivery, various formulation components have been investigated for their potential to facilitate the permeation of actives through the SC [28]. Furthermore, in the case of BC, various literatures reported that depending on the concentration of the solution, it can irritate in nasal sprays and eye drops; however, no irritation was observed in case of topical delivery [29]. In this study, based on *in vitro* permeability, NH-Tween-80 was observed as superior to NH-glycerol and NH-SLS. On the other hand, NH-Tween-80 also exhibited supremacy in drug release compared to conventional gel. This may have been due to the ensured static stabilization of ADP NH-Tween 80 by

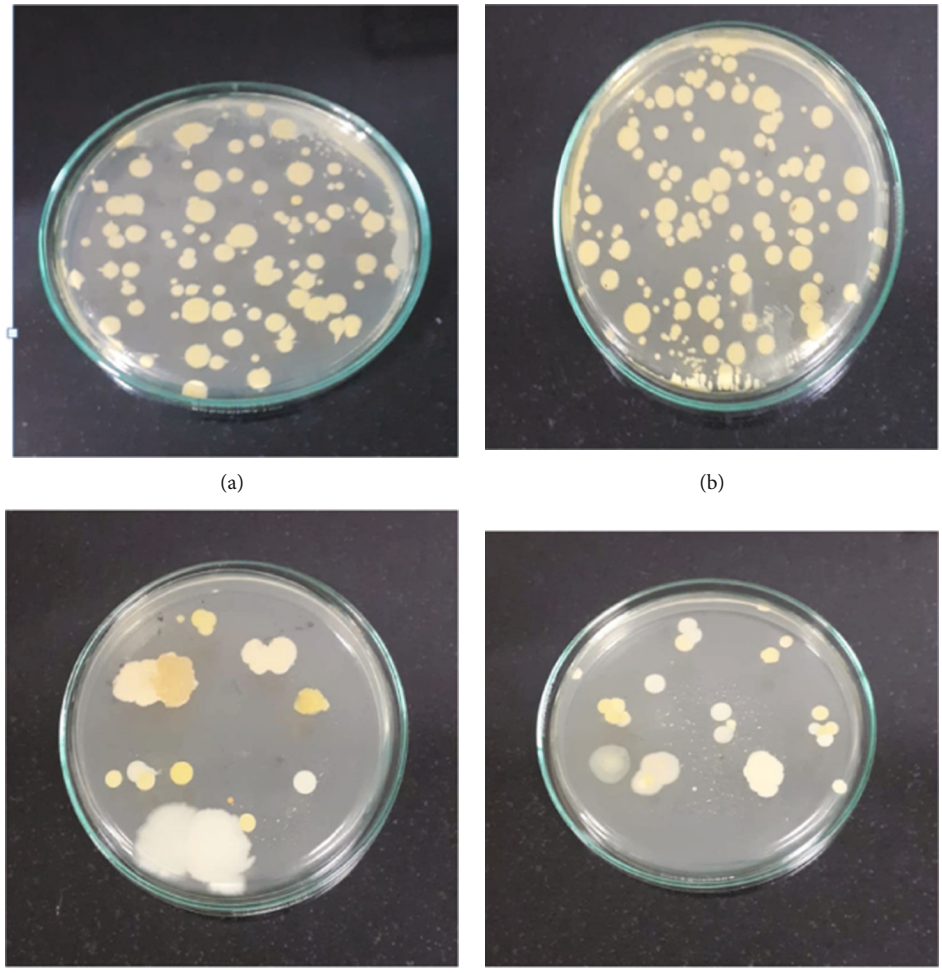

Figure 14: Dose-dependent effect of NH-Tween-80 against S. epidermidis: (a) 0.15 μg/mL, (b) 0.25 μg/mL, (c) 1.0 μg/mL, and (d) 1.25 μg/mL.

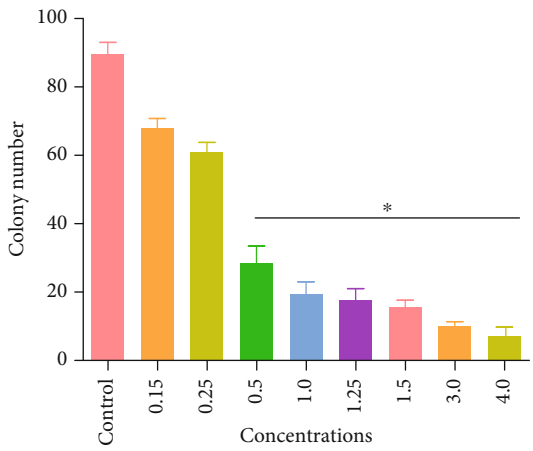

Figure 15: Antibacterial effect of NH-Tween-80 with different concentrations in μg/mL; $^{*}p < 0.05$ compared to control group.

comparatively bulkier (head), i.e., Tween-80 when compared to that of NH-glycerol or NH-SLS [26]. The overall *in vitro* and ex vivo permeability results are shown in Sections 7.1 and 7.2. On the other hand, in this study, the ADP-incorporated NH-Tween 80, NH-SLS, and NH-glycerol have sizes less than 100 nm; further, these droplets are dispersed in carbopol-940. Therefore, it could be addressed as nanogels or NHs. Previously, it has been reported that nanogels are nanoparticles composed of a hydrogel that is highly cross-linked physically or chemically with hydrophilic polymerchains [30]. Therefore, in our study, we have reported it as NH.

5.3. Particle Size, PDI, and Zeta Potential Evaluation. The NH-Tween-80 exhibited zeta size, PDI, and zeta potential of 76.53 ± 0.115 nm, 0.264 ± 0.312, −7.63 ± 1.12 mV, respectively. Furthermore, NH-SLS and NH-glycerol were demonstrated of zeta size 91.27 ± 0.257 and 84.59 ± 1.17 nm, respectively (Table 3). Among the three formulations, NH-Tween-80 revealed less particle size and PDI than NH-SLS and NH-glycerol. This is mainly due to the larger particle size where the value of PDI is too high. Similarly, small particle size demonstrates less PDI. This is because the PDI is directly proportional to the particle size [31]. All three formulations showed homogeneous droplet size distribution.

Table 5: NH-Tween-80.

Duration	Temp. (°C)	Humidity (%)	Assay[a] (%)	Transparency	Color change	pH[a]	Phase separation
1 day	25	NA	102.11 ± 0.22	+	—	5.31 ± 0.33	—
	40	75	101.78 ± 0.15	+	—	5.22 ± 0.10	—
1 month	25	NA	101.59 ± 0.37	+	—	5.41 ± 0.11	—
	40	75	101.42 ± 0.24	+	—	5.23 ± 0.12	—
3 months	25	NA	100.67 ± 0.17	+	—	5.38 ± 0.22	—
	40	75	100.06 ± 0.11	+	—	5.77 ± 0.18	—
6 months	25	NA	100.54 ± 0.31	+	—	5.55 ± 0.14	—
	40	75	99.25 ± 0.15	+	—	5.69 ± 0.08	—

[a]Values are expressed as mean ± SD ($n = 3$); +: presence; −: absence; NA: not applicable.

Table 6: NH-SLS.

Duration	Temp. (°C)	Humidity (%)	Assay[a] (%)	Transparency	Color change	pH[a]	Phase separation
1 day	25	NA	102.35 ± 0.11	+	—	5.34 ± 0.29	—
	40	75	102.29 ± 0.22	+	—	5.46 ± 0.31	—
1 month	25	NA	101.69 ± 0.24	+	—	5.31 ± 0.16	—
	40	75	99.12 ± 0.32	—	+	5.62 ± 0.33	—
3 months	25	NA	99.54 ± 0.22	—	—	6.02 ± 0.09	—
	40	75	94.13 ± 0.10	—	+	6.52 ± 0.11	—
6 months	25	NA	96.25 ± 0.09	—	+	5.88 ± 0.20	—
	40	75	91.23 ± 0.41	—	+	6.24 ± 0.10	—

[a]Values are expressed as mean ± SD ($n = 3$); +: presence; −: absence; NA: not applicable.

Table 7: NH-glycerol.

Duration	Temp. (°C)	Humidity (%)	Assay[a] (%)	Transparency	Color change	pH[a]	Phase separation
1 day	25	NA	102.51 ± 0.29	+	—	5.47 ± 0.27	—
	40	75	101.69 ± 0.11	+	—	5.51 ± 0.21	—
1 month	25	NA	102.36 ± 0.43	+	—	5.44 ± 0.25	—
	40	75	100.57 ± 0.41	—	—	5.37 ± 0.40	—
3 months	25	NA	101.10 ± 0.13	—	—	5.78 ± 0.06	—
	40	75	99.28 ± 0.12	—	+	5.67 ± 0.20	—
6 months	25	NA	99.23 ± 0.10	—	+	6.03 ± 0.19	—
	40	75	96.18 ± 0.20	—	+	6.31 ± 0.11	—

[a]Values are expressed as mean ± SD ($n = 3$); +: presence; −: absence; NA: not applicable.

A formulation with a value of PDI of approximately zero signifies droplet distribution in monodisperse manner. Similarly, PDI having almost one denotes a broad range of droplet distribution while having a 0.2 PDI value, exhibiting the distribution of homogeneous droplet size in NH-Tween-80, NH-SLS, and NH-glycerol [32]. All three NH formulations indicated a negative zeta potential value (from −7.63 ± 1.12 to −14.21 ± 1.67). A study done by Ribeiro and Ferrari and Rocha-Filho observed a remarkable negative value of zeta potentials with nonionic surfactants, and this phenomenon is linked with a few chemical characteristics of polyoxyethylene chains in the surfactants used [33, 34].

5.4. Evaluation of pH and Nanohydrogel Appearance. In this study, the pH of both the active phase and NH formulations was examined. Although there was minor variation in the pH of the active phase containing surfactants and cosurfactants (Figure 3), the overall pH value of all three NH formulations was almost the same. The NH-Tween-80, NH-SLS, and NH-glycerol exhibited pH values of 5.26, 5.30, and

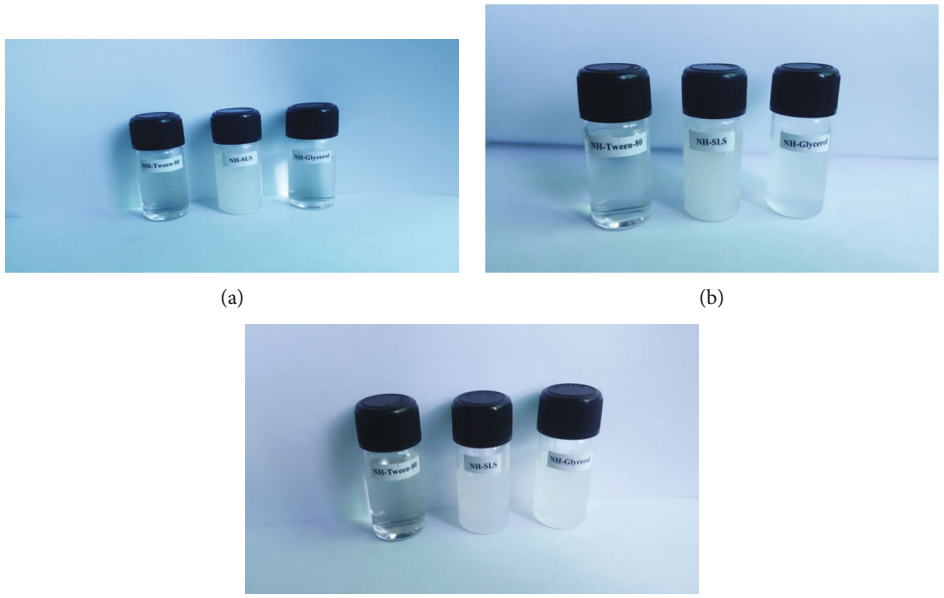

Figure 16: Photographs of ADP-optimized NH formulations in accelerated stability analysis: (a) 1st month, (b) 3rd month, and (c) 6th month.

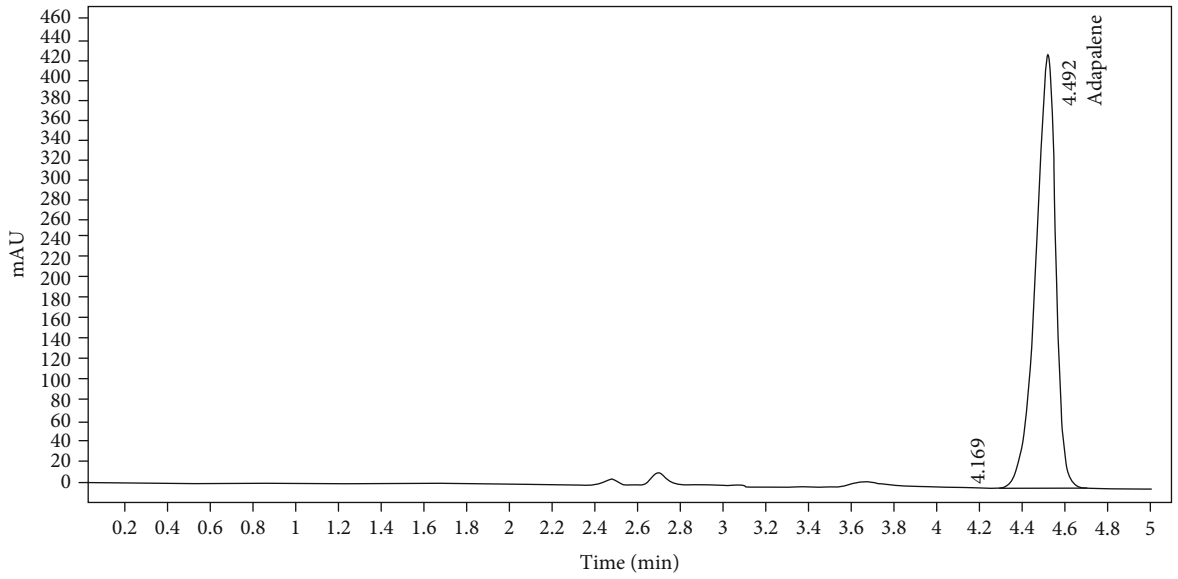

Figure 17: HPLC chromatograms of ADP standard solution (20 μg/mL).

5.46, respectively (Figure 4). The pH value of human skin ranges between 4.5 and 6.0, among which 5.5 is considered the average pH of human skin. Thus, the formulations targeted to apply to skin demonstrated the pH within the range of human skin pH [35]. The pH of formulations was not altered significantly over the 6th month at room temperature and accelerated stability. The formulated NHs were observed to be homogeneous and transparent and have a better consistency. The presence of any undissolved solid particles was not found (Figure 5). Moreover, as determined by TEM, optimized NH formulations' morphology and surface structure also suggested that all formulations were spherical (Figure 6).

5.5. Conductivity Analysis. The conductivity study was also assessed in ADP only containing surfactants and cosurfactants and NH formulations. The active phase containing SLS showed higher conductivity (26.91 μS/cm) followed by glycerol (24.6 μS/cm). The remaining surfactants and cosurfactants revealed approximately the same conductivity value (Figure 7). Furthermore, there was no noticeable difference in conductivity reading demonstrated by all NH

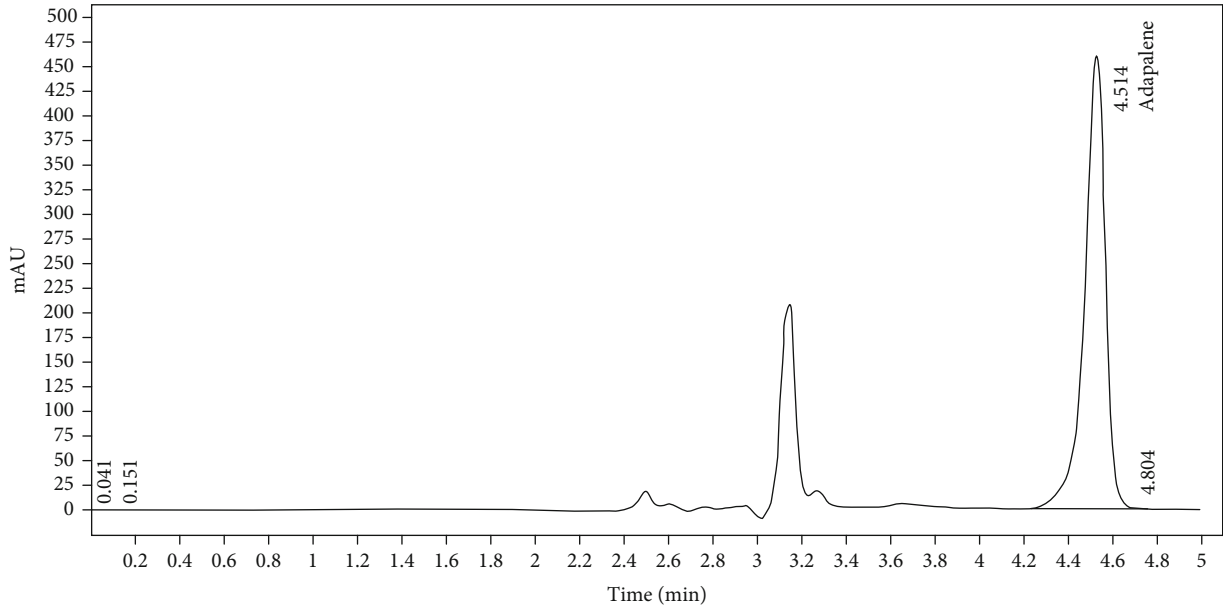

Figure 18: HPLC chromatograms of ADP NH-Tween-80 during initial analysis.

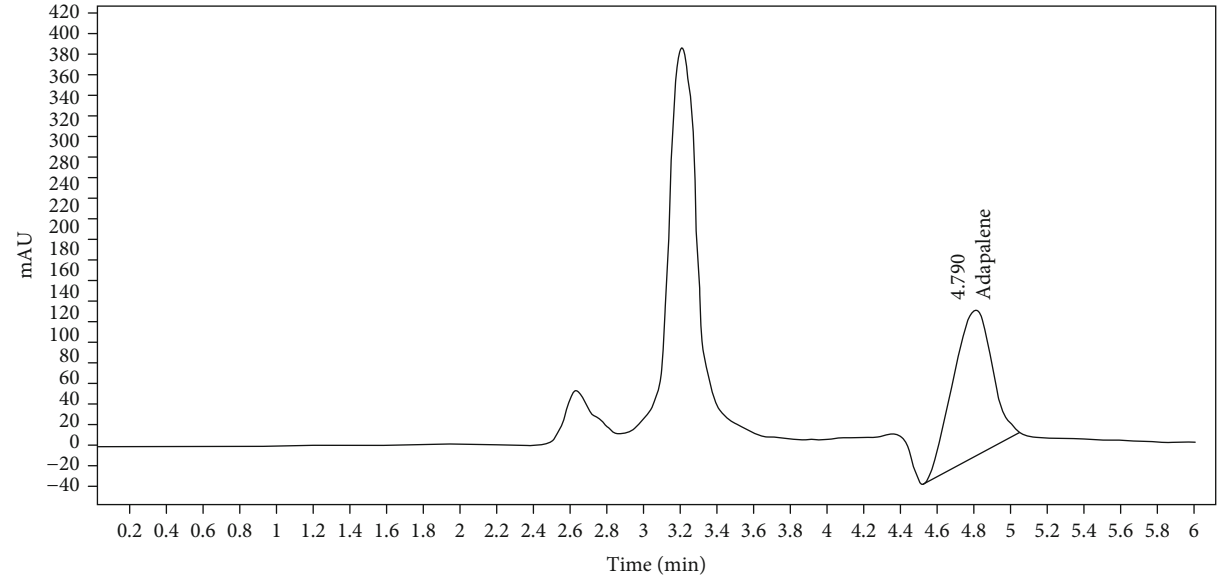

Figure 19: HPLC chromatograms of ADP NH-Tween-80 during the 6th month of accelerated stability analysis.

formulations (Figure 8). In addition, to determine the phase inversion, the assessment of electrical conductivity is very commonly used [36]. Although color was changed in the stability sample of H-SLS and H-glycerol, there was no significant change in conductivity. However, H-Tween-80 did not reveal any macroscopic destabilization signs of systems. It is reported that there are challenges to evaluating the stability of products solely by examining the conductivity because of having no direct relationship between the instability process and this parameter [37].

5.6. Viscosity and Spreadability Determination. The therapeutic efficacy of a topical gel formulation depends upon its potential to spread. Hence, spreadability estimation is a vital factor in determining the properties of topical application [38]. In this study, NH-Tween-80 revealed 7.5 ± 0.37 mm spreadability, higher than NH-SLS and NH-glycerol. Moreover, NH-Tween-80 also demonstrated viscosity of 2257 ± 0.41 cPs which was lower than other formulations (Table 4). The formulations having maximum viscosity showed the lowest spreadability. Furthermore, the NH preparations formulated using 0.66% carbopol-940 had a greater spreadability and lower viscosity than the formulation containing 0.70% and 0.75% carbopol-940. Moreover, to adequately permit the drug to be delivered through the skin, it is necessary to reveal appropriate spreading properties,

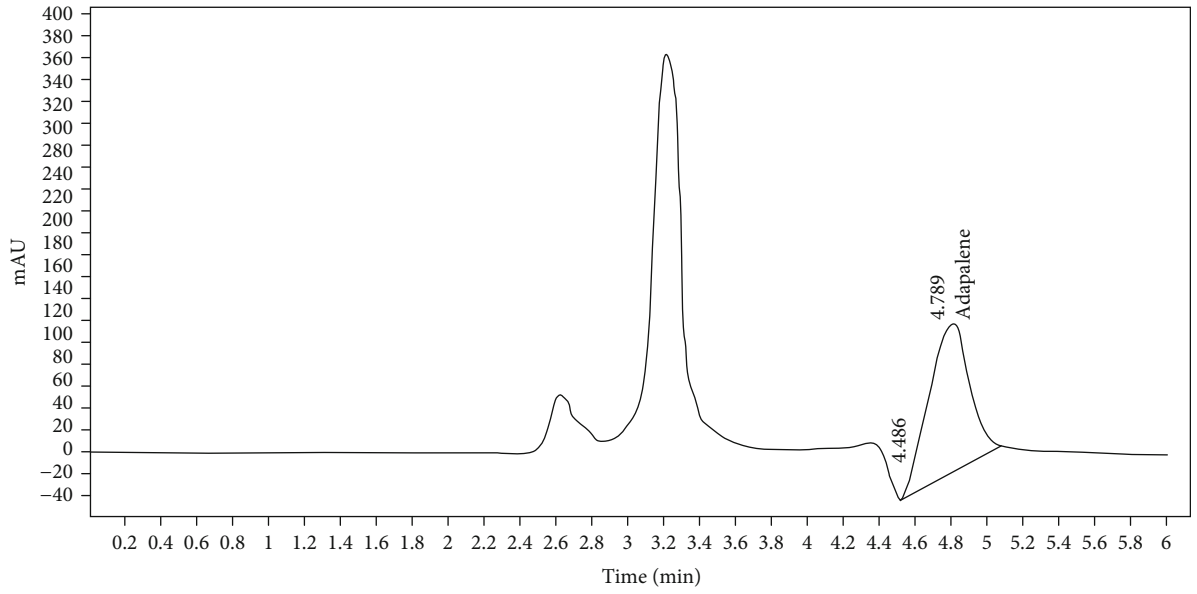

Figure 20: HPLC chromatograms of ADP NH-SLS during the 6th month of accelerated stability analysis.

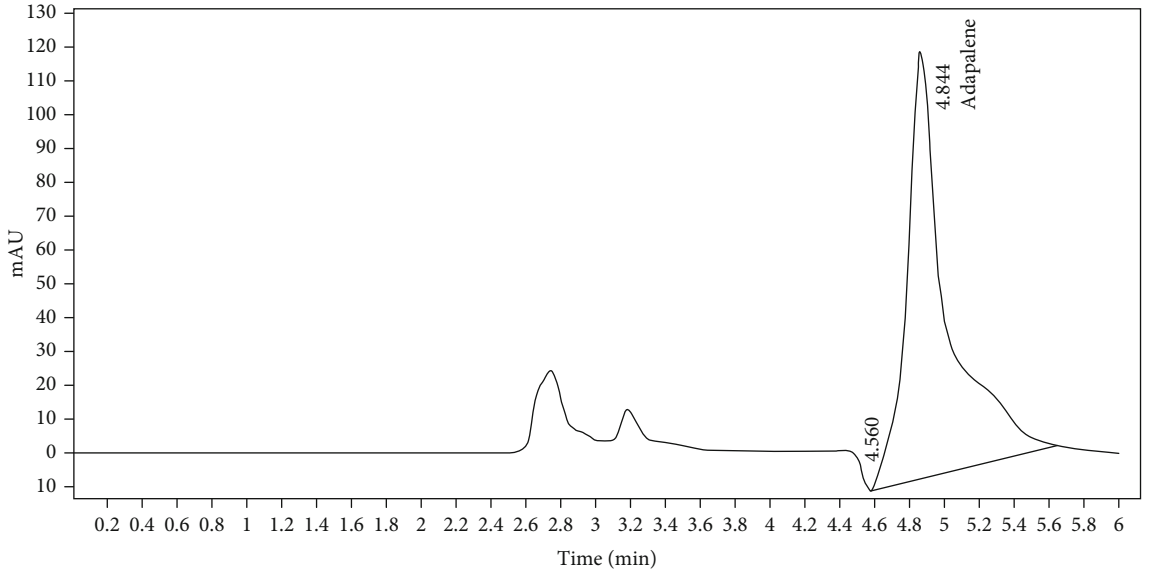

Figure 21: HPLC chromatograms of ADP NH-glycerol during the 6th month of accelerated stability analysis.

sufficient viscosity, and enhancing skin retention time by topical gel formulations [39]. In addition, it is suggested that the viscosity of the gel formulations is directly proportional to the concentration of the polymer [40].

5.7. Determination of ADP Assay in NH Formulations. The optimized NH formulations placed in room temperature ($25 \pm 2^{\circ}C$) and accelerated chamber ($25 \pm 2^{\circ}C$ and $75 \pm 5\%$ humidity) were analyzed on day 1. The NH formulations placed in room temperature showed ADP content $102.11\% \pm 0.22$, $102.35\% \pm 0.11$, and $102.51\% \pm 0.29$ in NH-Tween-80, NH-SLS, and NH-glycerol, respectively. Similarly, formulations stored in accelerated stability chambers demonstrated ADP value $101.78\% \pm 0.15$ (NH-Tween-80), $102.29\% \pm 0.22$ (NH-SLS), and $101.69\% \pm 0.11$ (NH-glycerol). All NH formulations revealed ADP percentage within the limit (90.0-110.0%). There was no significant difference in assay up to 6 months (Section 8).

6. Dermal Irritation Study

In this study, all optimized NH formulations and control samples have were not demonstrated any toxic reactions including redness, irritation, itching, inflammation, skin infection, or other injuries. All animals were found to be healthy, active, and alert, revealing no abnormal activities,

while for study carried out for observation, there was no rate of mortality.

7. Permeability Study

7.1. In Vitro Artificial Transdermal Membrane Permeability. The *in vitro* permeation behaviors of ADP in 0.3% DMSO (control solution), NH-Tween-80, NH-SLS, and NH-glycerol were examined over 24 h (Figure 9). In this study, NH-Tween-80 showed the drug permeability from 3 hrs of drug loading while NH-SLS, NH-glycerol, and ADP in 0.3% DMSO started to permeate from 6 hrs. At 24 h, NH-Tween-80 revealed 191.22 μg/mL of ADP permeation which was statistically significant ($p < 0.05$) compared with NH-SLS, NH-glycerol, and ADP in 0.3% DMSO. The p value obtained was 0.032, 0.037, and 0.003 for NH-Tween-80 vs. NH-SLS, NH-Tween-80 vs. NH-glycerol, and NH-Tween-80 vs. control solution, respectively. Moreover, the artificial membrane drug permeability of NH-Tween-80, NH-SLS, and NH-glycerol was enhanced by 6.93-, 3.35-, and 2.28-fold, respectively, compared with that of ADP in 0.3% DMSO. The specification of the European Medicines Agency draft regarding the quality of topical preparations and their equivalence was suggested in 2018 for appropriate utilization of synthetic membranes for proper understanding and activity characterizations of transdermal formulations [41]. Furthermore, these membranes are affordable and readily available in addition to better data reproducibility [42, 43]. Thus, in this study, Strat-M® was utilized as a diffusion membrane which is a synthetic membrane having several layers (300 μm thickness) homogeneous to the skin and composed of tightly packed multilayers of polyester sulfone. Various previously published papers used Strat-M® membrane to compare permeability potentiality of hydrophilic and lipophilic compounds such as diclofenac, hydrocortisone, caffeine, amphotericin B, and capsaicin. The data from different studies demonstrated that the Strat-M® membrane had a good interrelationship with human skin showing less variability, safety, and storage limitations [44–46].

To examine the impact of carbopol-940 on drug permeation, different ratios of carbopol-940 were studied. Among the three final NH formulations, NH-Tween-80 (F4) containing 0.66% carbopol-940 showed higher *in vitro* artificial membrane permeability as compared to 0.70% (F5) and 0.75% (F6) containing carbopol-940. In previous studies, the anionic surfactants like SLS hugely impede keratin and lipid bilayers of SC, changing the permeability of skin. These excipients are associated with uncoiling and extension of the helical filaments of the SC lipids. As a result, these modifications lead to enlargement in the membrane corresponding to increased permeability [47]. However, in this study, the permeability of NH-SLS was slightly lower than NH-glycerol. The permeation effect of H-SLS was probably hindered by the higher concentration of carbopol-940 in F6. This outcome might be justified with the formulation showing higher viscosity (Table 4). Low viscous preparations allow the drug for rapid movement compared to formulation consisting higher viscosity due to the reverse association between the drug release characteristics and viscosity [48].

This interconnection could alternate ADP delivering property from NH preparations. Therefore, phenomena of drug release from developed formulations rely on the dissolutions of hydrogels in aqueous media, and hydrogels with higher viscosity permit to emit ADP more gently compared to less viscous gels [49]. This consequence reveals that the hydrogel's viscosity plays a pivotal action role in controlling the rate of drug release, while diffusion of drug through the polymer matrix is a rate-determining step [50]. On the other hand, a molecule is also influenced by the physical characteristics of the polymer. Thermodynamic action and viscosity had an important impact on the release of an active component from the vehicle [51]. Furthermore, in this study, the drug permeation was directly proportional to the amount of ethanol. Formulations containing of 3.00% ethanol (F4) showed a higher ADP permeability as compared to formulations consisting 2.33% (F5) and 2.00% (F6) ethanol. To enhance the permeation of many drugs, ethanol is used as a cosolvent. It was known that ethanol promotes penetration via skin owing to its ability to disrupt the SC structure or promote the drug partitioning and solubility in SC [52].

7.2. Ex Vivo Drug Permeation. Human skin excised from cadavers or obtained from plastic surgeries is the appropriate model for assessment of *in vitro* absorption of drugs through the skin. However, human skin is not easily resourced, and animal models are often employed. The skin acquired from animal models is commonly suggested for preliminary evaluations in screening novel formulations. Guinea pigs, domestic pigs, rats, and mice are used as animal models to replace human skin [53]. The evaluation of permeation increasing activity of ADP on rat skin exhibits the application of natural membranes such as rat skin that is inevitable to estimate the release ability of drug [54]. The skin permeation profile of ADP from the DMSO solution and NH formulations is shown in Figure 10. The ex vivo concentration of drug release of ADP through rat skin was highest for NH-Tween-80 compared to NH-SLS, NH-glycerol, and ADP containing 0.3% DMSO solution. Furthermore, the results suggested that the permeation rate of ADP was enhanced remarkably ($p < 0.05$) for ADP-incorporated NH formulations as compared to ADP containing plain solution (0.3% DMSO). The obtained p value = 0.031, 0.037, and 0.027 for NH-Tween-80 vs. NH-SLS, NH-Tween-80 vs. NH-glycerol, and NH-Tween-80 vs. control solution, respectively. At 24 h, NH-Tween-80 revealed 305.11 μg/mL ADP permeation, which was 1.99-, 1.56-, and 4.89-fold greater than NH-SLS, NH-glycerol, and ADP incorporating 0.3% DMSO solution, respectively. Drug absorption of the percutaneous route is considered to exist in several skin parts such as hair follicles, sebaceous glands, and sweat ducts during the initial phase and the steady state. Generally, it is assumed that penetration enhancers like nonionic surfactants excrete into the intercellular lipid bilayers of skin therefore diminishing the crystalline characteristics of these lipid bilayers' crystallinity and intensifying their permeation potentiality [55]. Furthermore, the alternate mode of action associated with nonionic surfactants is the promotion of sebum emulsification and therefore elevate drug

thermodynamic activity [56, 57]. The prompt and higher ADP penetration via the skin is mainly because the formulation of NH-Tween-80 can elaborate with different mechanisms. Firstly, ADP adsorption and fusion over the skin surface result in a higher thermodynamic action gradient of drug at the interface. This phenomenon is a crucial step in the permeability of drugs. Secondly, permeation enhancer influences to decrease the barrier characteristics and modify the SC structure [58, 59]. Moreover, NH-Tween-80 exhibited a significantly higher ($p < 0.05$) ADP permeation in comparison with ADP conventional gel (p value = 0.036) and ADP containing 0.3% DMSO solution (p value = 0.024). At 24 h, the drug permeated by NH-Tween-80 was 3.38- and 4.89-fold higher than ADP conventional gel and ADP in 0.3% DMSO solution, respectively (Figure 11), which may be due to the particle size of the formulations. The nanosize of drugs may aid in elevating the bioavailability of poorly soluble compounds. The smaller particle size results in a greater surface area of particles, enhancing the drug amount available for permeation [60].

8. Antibacterial Effect of NH-Tween-80

Based on the results observed from the above experiments, the MIC of the NH-Tween-80 against standard strain of S. epidermidis (ATCC 12228) was examined. In this study, NH-Tween-80 demonstrated possibly remarkable growth inhibition against S. epidermidis with MIC of 0.50 μg/mL. Moreover, this formulation showed a significant dose-dependent antibacterial effect against S. epidermidis (Figure 12). Furthermore, the antibacterial effect of ADP-NH without adding Tween-80 as the control group was also carried out. However, this group revealed significant growth of bacteria as compared to NH formulation containing Tween-80 (Figure 13). This might be due to the penetration potentiality of Tween-80, which promoted the disruption of the bacterial cell wall and enhanced the permeation of ADP, which eventually demonstrated a remarkable role in inhibiting the growth of bacteria. In addition, to confirm the dose-dependent antibacterial effect of ADP NH-Tween-80 as a part of semiquantification, this formulation was further diluted before achieving a lower concentration of ADP. In this case, the lower concentration of this formulation (0.15 and 0.25 μg/mL) was not sufficiently inhibiting the bacterial growth. The impact of these concentrations was almost similar to the control group. Moreover, further enhancing this concentration at 1.0 and 1.25 μg/mL showed more impeding bacterial growth than the previous concentrations. However, no significant difference was observed between 0.5 and 1.0 μg/mL of concentration. Additionally, using concentrations higher than 1.0 μg/mL markedly hindered the bacteria growth. The bacterial growth inhibition effect of these concentrations is shown in Figure 14.

Furthermore, in this study, the antibacterial effect of ADP-incorporated NH-Tween-80 of various concentrations including control group was calculated by counting the colony forming units using colony counter. The overall obtained results are shown in Figure 15. Moreover, all concentrations revealed significant bacterial inhibition activity ($p < 0.05$) against control group except 0.15 and 0.25 μg/mL.

9. Accelerated Stability Analysis

The optimized three ADP-NH formulations were evaluated physically and chemically for six months in two different environmental conditions. The NH-Tween-80 demonstrated 99.25% ± 0.15 drug content in accelerated stability within the limit. This formulation was stable both physically and chemically, and there were no noticeable physical changes observed. The pH value was also within the skin pH range throughout the stability period (Table 5). In addition, during the 6th month of accelerated stability analysis, 91.23% ± 0.41 assay was observed in NH-SLS which was very close to the lower limit and decreased gradually. In this formulation, color change was observed within 1st month, and transparency of NH disappeared (Table 6). Hence, this formulation is considered as physically and chemically unstable. Moreover, NH-glycerol revealed 96.08% ± 0.20 drug content in the 6th month's accelerated analysis which was within the limit. However, color change was observed in the 3rd month of accelerated stability, and the rest of the parameters were obtained satisfactorily (Table 7). Thus, NH-glycerol was considered physically unstable but chemically stable. Furthermore, the photographs of three optimized formulations of ADP such as NH-Tween-80, NH-SLS, and NH-glycerol for the 1st, 3rd, and 6th months are shown in Figure 16. Moreover, the HPLC peak of ADP standard solution containing 20 μg/mL of concentration is demonstrated in Figure 17.

While examining the ADP in an accelerated stability analysis, the obtained retention time and total HPLC area were obtained almost same until 6 months (Figures 18–21) and compared to day 1 estimation which can also further justifies that ADP-loaded formulation is stable without significant degradation in potency despite of tolerating higher temperature and humidity in stability chamber.

10. Conclusions

Based on results obtained from this study, it can be concluded that ADP-NH containing Tween-80 (F4) can potentially enhance drug release. This formulation may be an optimistic carrier for topical administration of ADP to cure the acne vulgaris. This formulation revealed significantly higher *in vitro* and *ex vivo* ADP permeability compared to other NHs and conventional ADP gel formulations. The optimal formulation (NH-Tween-80) revealed 191.22 μg/mL of *in vitro* ADP permeation through Strat-M® membrane at 24 h. Moreover, this formulation demonstrated 305.11 μg/mL of ADP permeation in Wistar rat abdominal skin which was 1.99-, 1.56-, and 4.89-fold higher in comparison with NH-SLS, NH-glycerol, and control solution, respectively. Moreover, ex vivo permeability of NH-Tween-80 was also compared with conventional gel (commercially available sample), which was 3.38-fold greater at 24 h. Furthermore, no noticeable physical changes were observed, and drug content was found to be 99.25% ± 0.15 in NH

incorporating Tween-80 up to 6 months of accelerated stability analysis. These results may open a new approach for the remedies of acne vulgaris by topical application of ADP-NH. However, further adequate studies related to preclinical, clinical, and long-term stability are still necessary to endorse its efficiency declaration in humans.

Data Availability

The data obtained from this study were presented in the form of figures and tables in the manuscript.

Conflicts of Interest

The authors declare that they have no conflicts of interest.

Acknowledgments

The authors are thankful to Asian Pharmaceuticals, Rupandehi, Nepal, for providing the opportunity to conduct this research. In addition, the authors are also grateful to Sunsari Technical College, Dharan, Sunsari, Nepal, for administering access to carry out animal experiments.

References

[1] J. Ayer and N. Burrows, "Acne: more than skin deep," *Postgraduate Medical Journal*, vol. 82, no. 970, pp. 500–506, 2006.

[2] J. Leyden, L. Stein-Gold, and J. Weiss, "Why topical retinoids are mainstay of therapy for acne," *Dermatology and Therapy*, vol. 7, no. 3, pp. 293–304, 2017.

[3] A. Rusu, C. Tanase, G. A. Pascu, and N. Todoran, "Recent Advances Regarding the Therapeutic Potential of Adapalene," *Pharmaceuticals*, vol. 13, no. 9, p. 217, 2020.

[4] J. S. Weiss, D. M. Thiboutot, J. Hwa, Y. Liu, and M. Graeber, "Long-term safety and efficacy study of adapalene 0.3% gel," *Journal of Drugs in Dermatology*, vol. 7, 6 Suppl, pp. s24–s28, 2008.

[5] A. K. Jain, A. Jain, N. K. Garg et al., "Adapalene loaded solid lipid nanoparticles gel: an effective approach for acne treatment," *Colloids and Surfaces. B, Biointerfaces*, vol. 121, pp. 222–229, 2014.

[6] R. Najafi-Taher, B. Ghaemi, and A. Amani, "Delivery of adapalene using a novel topical gel based on tea tree oil nanoemulsion: permeation, antibacterial and safety assessments," *European Journal of Pharmaceutical Sciences*, vol. 120, pp. 142–151, 2018.

[7] J. R. Antonio, C. R. Antonio, I. L. S. Cardeal, J. M. A. Ballavenuto, and J. R. Oliveira, "Nanotechnology in dermatology," *Anais Brasileiros de Dermatologia*, vol. 89, no. 1, pp. 126–136, 2014.

[8] M. Schneider, F. Stracke, S. Hansen, and U. F. Schaefer, "Nanoparticles and their interactions with the dermal barrier," *Dermato-endocrinology*, vol. 1, no. 4, pp. 197–206, 2009.

[9] A. C. Lauer, L. M. Lieb, C. Ramachandran, G. L. Flynn, and N. D. Weiner, "Transfollicular drug delivery," *Pharmaceutical Research*, vol. 12, no. 2, pp. 179–186, 1995.

[10] S. K. Jain, A. Verma, A. Jain, and P. Hurkat, "Transfollicular drug delivery: current perspectives," *Research and Reports in Transdermal Drug Delivery*, vol. 5, pp. 1–17, 2016.

[11] X. Li, H. Sun, H. Li et al., "Multi-responsive biodegradable cationic nanogels for highly efficient treatment of tumors," *Advanced Functional Materials*, vol. 31, no. 26, p. 2100227, 2021.

[12] Y. F. Ding, J. Wei, S. Li, Y. T. Pan, L. H. Wang, and R. Wang, "Host-guest interactions initiated supramolecular chitosan nanogels for selective intracellular drug delivery," *ACS Applied Materials & Interfaces*, vol. 11, no. 32, pp. 28665–28670, 2019.

[13] Y. Luo, X. Wei, Y. Wan, X. Lin, Z. Wang, and P. Huang, "3D printing of hydrogel scaffolds for future application in photothermal therapy of breast cancer and tissue repair," *Acta Biomaterialia*, vol. 92, pp. 37–47, 2019.

[14] P. Ghasemiyeh and S. Mohammadi-Samani, "Potential of nanoparticles as permeation enhancers and targeted delivery options for skin: advantages and disadvantages," *Drug Design, Development and Therapy*, vol. Volume 14, pp. 3271–3289, 2020.

[15] L. Sun, Z. Liu, L. Wang et al., "Enhanced topical penetration, system exposure and anti-psoriasis activity of two particle-sized, curcumin-loaded PLGA nanoparticles in hydrogel," *Journal of Controlled Release*, vol. 254, pp. 44–54, 2017.

[16] S. Kalepu and V. Nekkanti, "Insoluble drug delivery strategies: review of recent advances and business prospects," *Acta Pharmaceutica Sinica B*, vol. 5, no. 5, pp. 442–453, 2015.

[17] M. X. Chen, K. S. Alexander, and G. Baki, "Formulation and Evaluation of Antibacterial Creams and Gels Containing Metal Ions for Topical Application," *Journal of Pharmaceutics*, vol. 2016, Article ID 5754349, 10 pages, 2016.

[18] V. Sabale, H. Kunjwani, and P. Sabale, "Formulation and in vitro evaluation of the topical antiageing preparation of the fruit of Benincasa hispida," *Journal of Ayurveda and Integrative Medicine*, vol. 2, no. 3, pp. 124–128, 2011.

[19] United States Pharmacopeial, C, *The United States Pharmacopeia, USP 41/ The national formulary : NF*, US Pharmacopeial Convention, 2018.

[20] S. N. Nair, M. S. Nair, D. Nair et al., "International Journal of Biological & Pharmaceutical Research Wound Healing, Anti Inflammatory Activity and Toxicological Studies of Leea asiatica (L.) Ridsdale," *International Journal of Biological & Pharmaceutical Research*, vol. 5, pp. 745–749, 2014.

[21] G. S. Njateng, D. Gatsing, R. S. Mouokeu, P. K. Lunga, and J. R. Kuiate, "In vitro and in vivo antidermatophytic activity of the dichloromethane-methanol (1:1 v/v) extract from the stem bark of Polyscias fulva Hiern (Araliaceae)," *BMC Complementary and Alternative Medicine*, vol. 13, no. 1, p. 95, 2013.

[22] L. Subedi, S.-Y. Song, S. K. Jha et al., "Preparation of topical itraconazole with enhanced skin/nail permeability and in vivo antifungal efficacy against superficial mycosis," *Pharmaceutics*, vol. 13, no. 5, p. 622, 2021.

[23] N. Gemeda, A. Tadele, H. Lemma et al., "Development, characterization, and evaluation of novel broad-spectrum antimicrobial topical formulations from Cymbopogon martini (Roxb.) W. Watson essential oil," *Evidence-based Complementary and Alternative Medicine*, vol. 2018, Article ID 9812093, 16 pages, 2018.

[24] M. S. Muthu and S.-S. Feng, "Pharmaceutical stability aspects of nanomedicines," *Nanomedicine*, vol. 4, no. 8, pp. 857–860, 2009.

[25] D. A. Dri, C. Marianecci, M. Carafa, E. Gaucci, and D. Gramaglia, "Surfactants, nanomedicines and nanocarriers:

a critical evaluation on clinical trials," *Pharmaceutics*, vol. 13, no. 3, p. 381, 2021.

[26] X. Li, Y. Qin, C. Liu, S. Jiang, L. Xiong, and Q. Sun, "Size-controlled starch nanoparticles prepared by self-assembly with different green surfactant: the effect of electrostatic repulsion or steric hindrance," *Food Chemistry*, vol. 199, pp. 356–363, 2016.

[27] V. P. Chavda and D. Shah, "Self-emulsifying delivery systems: One step ahead in improving solubility of poorly soluble drugs," *Nanostructures for Cancer Therapy*, pp. 653–718, 2017.

[28] Y. Zhang, M. E. Lane, and D. J. Moore, "An investigation of the influence of PEG 400 and PEG-6-Caprylic/capric glycerides on dermal delivery of niacinamide," *Polymers (Basel)*, vol. 12, no. 12, p. 2907, 2020.

[29] B. Merchel Piovesan Pereira and I. Tagkopoulos, "Benzalkonium chlorides: uses, regulatory status, and microbial resistance," *Applied and Environmental Microbiology*, vol. 85, no. 13, 2019.

[30] A. Mohapatra, S. Uthaman, and I.-K. Park, *Chapter 10 - Polyethylene glycol nanoparticles as promising tools for anticancer therapeutics, in polymeric nanoparticles as a promising tool for anti-cancer therapeutics*, P. Kesharwani, K. M. Paknikar, and V. Gajbhiye, Eds., Academic Press, 2019.

[31] P. Kaur, T. Garg, G. Rath, R. S. Murthy, and A. K. Goyal, "Development, optimization and evaluation of surfactant-based pulmonary nanolipid carrier system of paclitaxel for the management of drug resistance lung cancer using Box-Behnken design," *Drug Delivery*, vol. 23, no. 6, pp. 1912–1925, 2016.

[32] S. Y. Tang, S. Manickam, T. K. Wei, and B. Nashiru, "Formulation development and optimization of a novel Cremophore EL-based nanoemulsion using ultrasound cavitation," *Ultrasonics Sonochemistry*, vol. 19, no. 2, pp. 330–345, 2012.

[33] R. C. Ribeiro, S. Barreto, E. Ostrosky, P. Rocha-Filho, L. Veríssimo, and M. Ferrari, "Production and characterization of cosmetic nanoemulsions containing Opuntia ficus-indica (L.) mill extract as moisturizing agent," *Molecules*, vol. 20, no. 2, pp. 2492–2509, 2015.

[34] M. Ferrari and P. Rocha-Filho, "Multiple emulsions containing amazon oil: açaí oil (Euterpe oleracea)," *Revista Brasileira de Farmacognosia*, vol. 21, no. 4, pp. 737–743, 2011.

[35] A. Naveed, "Anti-aging potential of a cream containing milk thistle extract: formulation and in vivo evaluation," *African Journal of Biotechnology*, vol. 11, 2012.

[36] J. Jiang, Z. Mei, J. Xu, and D. Sun, "Effect of inorganic electrolytes on the formation and the stability of water-in-oil (W/O) emulsions," *Colloids and Surfaces A: Physicochemical and Engineering Aspects*, vol. 429, pp. 82–90, 2013.

[37] D. S. Bernardi, T. A. Pereira, N. R. Maciel et al., "Formation and stability of oil-in-water nanoemulsions containing rice bran oil: in vitro and in vivo assessments," *Journal of Nanobiotechnology*, vol. 9, no. 1, p. 44, 2011.

[38] S. Lakshmana Prabu, S. Arun, S. Annie, and K. Aravind, "Evaluation of rosin as a cream base for topical ketoconazole preparation," *Journal of Pharmaceutical Research*, vol. 8, pp. 89–92, 2015.

[39] H. M. Lin, L. Lin, M. Sun, J. Liu, and Q. Wu, "Topical delivery of four neuroprotective ingredients by ethosome-gel: synergistic combination for treatment of oxaliplatin-induced peripheral neuropathy," *International Journal of Nanomedicine*, vol. Volume 15, pp. 3251–3266, 2020.

[40] M. Shukr and G. Metwally, "Evaluation of topical gel bases formulated with various essential oils for antibacterial activity against methicillin-resistant Staphylococcus aureus," *Tropical Journal of Pharmaceutical Research*, vol. 12, pp. 877–884, 2014.

[41] P. K. Bolla, B. A. Clark, A. Juluri, H. S. Cheruvu, and J. Renukuntla, "Evaluation of formulation parameters on permeation of ibuprofen from topical formulations using Strat-M(®) membranes," *Pharmaceutics*, vol. 12, no. 2, p. 151, 2020.

[42] S. Zsikó, Csányi, Kovács, Budai-Szűcs, Gácsi, and Berkó, "Methods to evaluate skin penetration in vitro," *Scientia Pharmaceutica*, vol. 87, no. 3, p. 19, 2019.

[43] S. Nallagundla, S. Patnala, and I. Kanfer, "Comparison of in vitro release rates of acyclovir from cream formulations using vertical diffusion cells," *AAPS PharmSciTech*, vol. 15, no. 4, pp. 994–999, 2014.

[44] A. Haq, M. Dorrani, B. Goodyear, V. Joshi, and B. Michniak-Kohn, "Membrane properties for permeability testing: skin versus synthetic membranes," *International Journal of Pharmaceutics*, vol. 539, no. 1-2, pp. 58–64, 2018.

[45] L. Kaur, K. Singh, S. Paul, S. Singh, S. Singh, and S. K. Jain, "A mechanistic study to determine the structural similarities between artificial membrane Strat-M™ and biological membranes and its application to carry out skin permeation study of amphotericin B nanoformulations," *AAPS PharmSciTech*, vol. 19, no. 4, pp. 1606–1624, 2018.

[46] J. H. Kim, J. A. Ko, J. T. Kim et al., "Preparation of a capsaicin-loaded nanoemulsion for improving skin penetration," *Journal of Agricultural and Food Chemistry*, vol. 62, no. 3, pp. 725–732, 2014.

[47] A. Pandey, "Role of surfactants as penetration enhancer in transdermal drug delivery system," *Journal of Molecular Pharmaceutics & Organic Process Research*, vol. 2, no. 2, 2014.

[48] A. Babar, R. D. Bhandari, and F. M. Plakogiannis, "In-vitro release studies op chlorpheniramine maleate from topical bases using cellulose membrane and hairless mouse skin," *Drug Development and Industrial Pharmacy*, vol. 17, no. 8, pp. 1027–1040, 1991.

[49] E. J. Ricci, M. V. L. B. Bentley, M. Farah, R. E. S. Bretas, and J. M. Marchetti, "Rheological characterization of Poloxamer 407 lidocaine hydrochloride gels," *European Journal of Pharmaceutical Sciences*, vol. 17, no. 3, pp. 161–167, 2002.

[50] J. Y. Fang, T. L. Hwang, and Y. L. Leu, "Effect of enhancers and retarders on percutaneous absorption of flurbiprofen from hydrogels," *International Journal of Pharmaceutics*, vol. 250, no. 2, pp. 313–325, 2003.

[51] C. Tas, C. K. Ozkan, A. Savaser, Y. Ozkan, U. Tasdemir, and H. Altunay, "Nasal absorption of metoclopramide from different Carbopol® 981 based formulations: In vitro, ex vivo and in vivo evaluation," *European Journal of Pharmaceutics and Biopharmaceutics*, vol. 64, no. 2, pp. 246–254, 2006.

[52] S. A. Al-Suwayeh, E. I. Taha, F. M. Al-Qahtani, M. O. Ahmed, and M. M. Badran, "Evaluation of skin permeation and analgesic activity effects of carbopol lornoxicam topical gels containing penetration enhancer," *The Scientific World Journal*, vol. 2014, Article ID 127495, 9 pages, 2014.

[53] M. K. Nair, D. J. Chetty, Y. W. Chien, and H. Ho, "Biomembrane permeation of nicotine: mechanistic studies with porcine mucosae and skin," *Journal of Pharmaceutical Sciences*, vol. 86, no. 2, pp. 257–262, 1997.

[54] H. K. Vaddi, P. C. Ho, and S. Y. Chan, "Terpenes in propylene glycol as skin-penetration enhancers: permeation and

partition of haloperidol, Fourier transform infrared spectroscopy, and differential scanning calorimetry," *Journal of Pharmaceutical Sciences*, vol. 91, no. 7, pp. 1639–1651, 2002.

[55] K. Zhao, S. Singh, and J. Singh, "Effect of menthone on the in vitro percutaneous absorption of tamoxifen and skin reversibility," *International Journal of Pharmaceutics*, vol. 219, no. 1-2, pp. 177–181, 2001.

[56] P. C. Wu, Y. B. Huang, J. Y. Fang, and Y. H. Tsai, "Percutaneous absorption of captopril from hydrophilic cellulose derivatives through excised rabbit skin and human skin," *Drug Development and Industrial Pharmacy*, vol. 24, no. 2, pp. 179–182, 1998.

[57] L. Subedi, P. Pandey, J. H. Shim et al., "Preparation of topical bimatoprost with enhanced skin infiltration and in vivo hair regrowth efficacy in androgenic alopecia," *Drug Delivery*, vol. 29, no. 1, pp. 328–341, 2022.

[58] B. Vora, A. J. Khopade, and N. K. Jain, "Proniosome based transdermal delivery of levonorgestrel for effective contraception," *Journal of Controlled Release*, vol. 54, no. 2, pp. 149–165, 1998.

[59] J. Y. Fang, S. Y. Yu, P. C. Wu, Y. B. Huang, and Y. H. Tsai, "In vitro skin permeation of estradiol from various proniosome formulations," *International Journal of Pharmaceutics*, vol. 215, no. 1-2, pp. 91–99, 2001.

[60] K. Moribe, M. Shibata, T. Furuishi, K. Higashi, K. Tomono, and K. Yamamoto, "Effect of particle size on skin permeation and retention of piroxicam in aqueous suspension," *Chemical and Pharmaceutical Bulletin*, vol. 58, no. 8, pp. 1096–1099, 2010.